MEASURING GEOMETRICAL OUT-OF-PLANE IMPERFECTIONS IN STEEL TIED ARCH BRIDGES

Amelie Outtier
Ghent University, Belgium

Hans De Backer
Ghent University, Belgium

Bart De Pauw
Ghent University, Belgium

Philippe Van Bogaert
Ghent University, Belgium

The structural behavior of steel tied arch bridges is determined by the introduction of a large compressive force. As a consequence, slender steel arches are highly sensitive to in-plane as well as out-of-plane buckling. At present, no specific buckling curves for out-of-plane buckling exist for non-linear or curved elements in the international codes and calculation methods. Hence, the buckling curves for straight columns, as determined by ECCS are used, which leads to considerable inaccuracies in the assessment of the critical buckling load for arch bridges.

This paper is mainly concerned with quantifying the geometrical imperfection of real arch bridges based on the results of on-site strain measurements of the arches. Six bridges in total have been equipped with strain gauges along their entire length. For the actual determination of the imperfection, a detailed finite element model has been developed, describing all internal forces in an arch bridge, such as normal force, in-plane and out-of-plane bending and torsion, separately. In addition, the detailed model takes the influence of deformations on the internal forces into account.

This method is verified using the results of topographical measurements of some of the studied bridges. Both sets of results are in agreement when it comes to size and shape of the imperfections. The shape of the resulting geometrical imperfection is for most of these bridges a half sine wave. The most important result is however that for all bridges the size of the imperfections is substantially smaller than the one predicted by the Eurocodes.

Corresponding author's email: Hans.DeBacker@UGent.be

MEASURING GEOMETRICAL OUT-OF-PLANE IMPERFECTIONS IN STEEL TIED ARCH BRIDGES

First Amelie Outtier[1], Hans De Backer[1], Bart De Pauw[1] and Philippe Van Bogaert[1]

[1] Civil Engineering Department, Ghent University, Ghent, Belgium

ABSTRACT: The structural behavior of steel tied arch bridges is determined by the introduction of a large compressive force. As a consequence, slender steel arches are highly sensitive to in-plane as well as out-of-plane buckling. At present, no specific buckling curves for out-of-plane buckling exist for non-linear or curved elements in the international codes and calculation methods. Hence, the buckling curves for straight columns, as determined by ECCS are used, which leads to considerable inaccuracies in the assessment of the critical buckling load for arch bridges. This paper is mainly concerned with quantifying the geometrical imperfection of real arch bridges based on the results of on-site strain measurements of the arches. Six bridges in total have been equipped with strain gauges along their entire length. For the actual determination of the imperfection, a detailed finite element model has been developed, describing all internal forces in an arch bridge, such as normal force, in-plane and out-of-plane bending and torsion, separately. In addition, the detailed model takes the influence of deformations on the internal forces into account. This method is verified using the results of topographical measurements of some of the studied bridges. Both sets of results are in agreement when it comes to size and shape of the imperfections. The shape of the resulting geometrical imperfection is for most of these bridges a half sine wave. The most important result is however that for all bridges the size of the imperfections is substantially smaller than the one predicted by the Eurocodes.

1 INTRODUCTION

A recently built bridge across the Albert Canal in Antwerp (Belgium) was used as a testing case for the following calculations (Figure 1). This bridge is part of the high-speed railway connection between Antwerp and Amsterdam. The bridge span equals 115m, which apparently is quite larger than the actual canal itself. However this span was chosen in view of the future widening of the canal. The two lateral arches are connected to the lower chord edge members by 16 inclined hangers. The upper bracing comprises 3 tubes of large diameter. The arch springs are tied by the lower chord, consisting of a steel orthotropic deck plate. At the nodes, connecting the arches to the hangers, diaphragms have been provided to prevent distortion and introduce the hanger

forces. The arch sections, connected to the tube bracings are also equipped with stiffening diaphragms.

In order to verify the buckling resistance of the bridge, a refined FE-model of the bridge has been developed. During loading tests with lorries, strain measurements were carried out. These have been used for the on-going research.

Figure 1. High-speed railway bridge across the Albert Canal, Antwerp, Belgium.

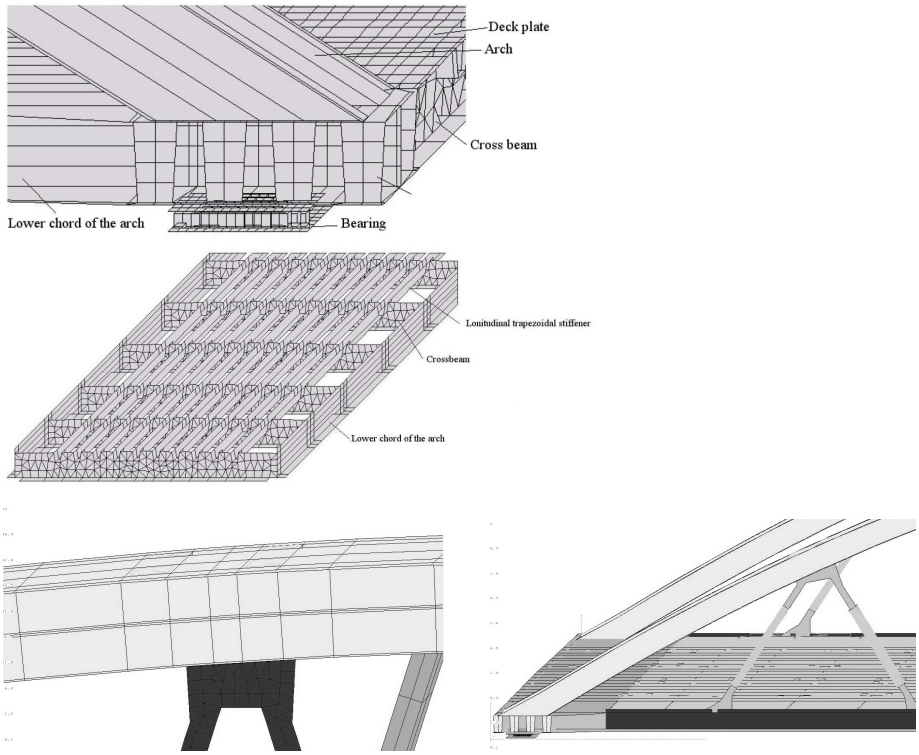

Figure 2. Details of FE-model.

2 FINITE ELEMENT MODELLING

2.1 Model description

Except for the bearings, the bridge model is constructed of nearly 50.000 Mindlin shell elements. The elements used allow taking into account shear deformations of thick shells. All parts of the arches, the hangers, the connections between the hangers and arches, the diaphragms and the bracings have been modeled in detail.

Special attention was given to the bearings and the connection between the arch springs and the lower chord edge members. A first calculation run of the model has shown that a torsional effect exists at the arch springs, this fading rapidly with increasing distance to the springs. Torsion is introduced by the neoprene bearings, which are not completely identical for the two arches, resulting in unsymmetrical end conditions. A neoprene bearing, for which the movement in restrained transversely, can still move a millimeter in that direction. The same applies to the longitudinally and the fully restrained bearings. This necessitates the use of approximately 2000 volume elements. A flexible/flexible contact between the neoprene and the fixing studs has been assumed. For this, a contact element has been created, with a kinematic constraint that is active when contact occurs and inactive without contact conditions. Figure 2 shows some detailed views of the used finite element model: the connection of arch to stringer, the deck plate , the detailed element model of the hanger to arch connection and finally a detailed view of overall concept.

2.2 Application of the model

The use of the finite element model is twofold. On one hand, it is used to re-calculate a given imperfection. On the other hand, the model enables to find the buckling curve of an arch with imperfections according to Van Bogaert et al (2005).

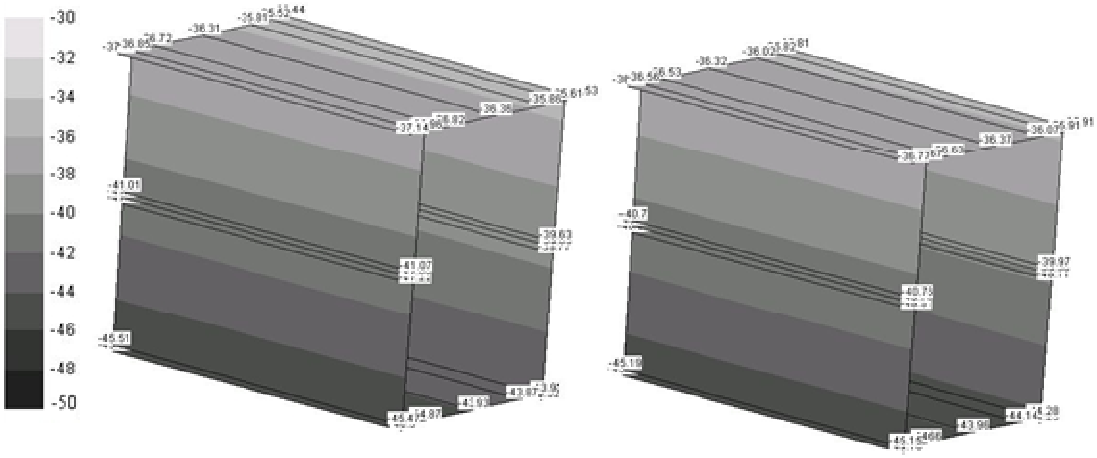

Figure 3. Stresses with and without imperfection.

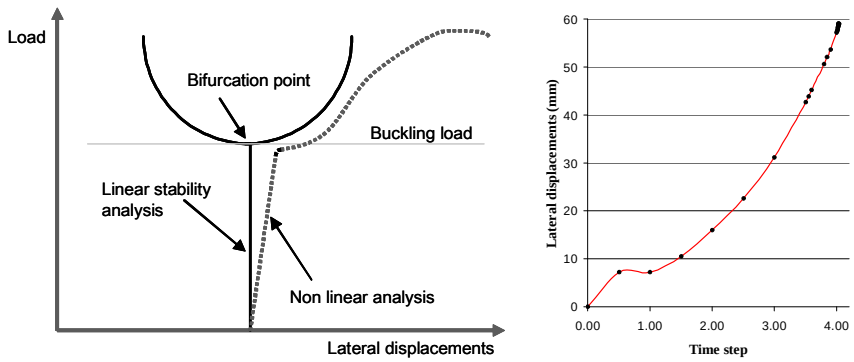

Figure 4. Theoretical buckling curve (left) and lateral displacement (mm) of middle arch section (right).

Figure 3 shows the same section of the perfect arch (left) and of the arch having sinusoidal imperfections with amplitude of a magnitude of 5 mm added to the perfect arch geometry. Comparing both results, clearly demonstrates that the imperfections cause changes in the stress field in the arch. The analytical method described in the following paragraphs is based on this fact. To calculate buckling curves, elastic-plastic analysis has been preferred to linear stability assessment. This allows, as shown in Figure 4 left, to distinguish the lateral displacement increase with increments of the load before reaching the bifurcation point. In contrast to a linear stability analysis, a non-linear analysis returns the failure load of the construction. A secondary advantage of the procedure is that not all loads are increased during the analysis, for example the dead load remaining constant during the increasing process. Figure 6b shows the increasing lateral displacements during rising of the live loads. Live loads are increased along a linear path until the calculation was ended after 4.05 seconds because of non-convergence issues in the software caused by the increasing displacements because of the buckling of the arch. This implies that live loads can be multiplied by a factor of 4.05 after full dead and live load are achieved before lateral buckling occurs.

2.3 Experimental procedure

The internal stresses, following from finite element calculations, are compared to the stresses measured during loading tests in the bridge of the Albert Canal. This allowed assessment of the Albert Canal bridge imperfections, as a typical example of steel tied arch bridges.

The test load consisted of 18 calibrated lorries. For various positions of the lorries, strains have been measured at the 4 edges of the cross section, in 6 different measurement sections across the span as displayed in Figure 7. Since the strain gauges were applied after the construction of the bridge, the strains recorded concern the live load effects only, the dead load not having to appear in the analytical calculations.

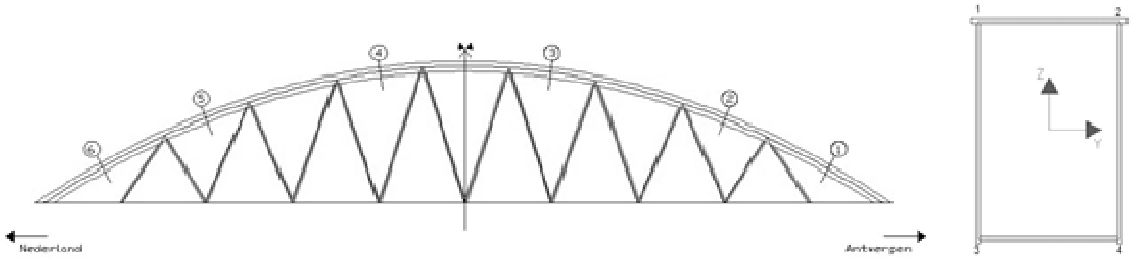

Figure 5. Location of the measurement sections.

3 METHODOLOGY

It is assumed that the geometrical out-of-plane imperfections of steel tied arch follow a more or less piecewise continuous behavior, due to the production process (welding process, assembly of the cross-section, assembly of the arch, etc.) of the arch section. In addition, the assembly of the arch will lead to all geometrical imperfections having a much localized character, specifically in the regions where the different parts of the arch are connected. Although localized by nature, the imperfections will influence the overall stress field in the entire arch.

The geometrical imperfection is furthermore assumed to be identical in all points within the same arch cross-section. Small differences can occur in reality, because of limited displacements and rotations, but the overall size is neglectable when compared with the size of the actual imperfections. Thus, if the considered arch is equipped with strain gauges in n cross-sections along its length, only n unknown geometrical imperfections have to be calculated: δ_1, δ_2, …, δ_n. The geometrical imperfections in all other cross-sections are neglected since the number of considered cross-sections is high enough to get a good approximation of the imperfections. The influence of imperfections in all other cross-sections is implicitly part of the method.

A relation has to be found between the measured stresses and the actual imperfections. All measured stresses do not only include the influence of the imperfections but also the normal force and in- and out-of-plane bending moments due to the live load on the bridge. The stresses caused by the out of plane imperfections are determined by subtracting the stresses due to the normal behavior of a perfect arch, as calculated using the detailed finite element models discussed before.

In order to formulate a correlation of the unique geometrical imperfection in a certain cross-section and the corresponding change of the stresses in the arch, it is postulated that the influence of out-of-plane imperfections is comparable to the effect of an additional out-of-plane bending moment. This additional bending moment is caused by the fact that the normal forces in the arch cross-section will act excentrically because of the imperfection. Thus, a correlation will be determined between the unknown geometrical imperfections, δ_1, δ_2, …, δ_n., and the stresses, σ_1, σ_2, …, σ_n, defined as the difference between the mean stresses in both flanks of the arch cross-section:

$$\begin{pmatrix} \sigma_1 \\ \vdots \\ \sigma_i \\ \vdots \\ \sigma_n \end{pmatrix} = (H) . \begin{pmatrix} \delta_1 \\ \vdots \\ \delta_i \\ \vdots \\ \delta_n \end{pmatrix} \tag{1}$$

The values of the matrix, [H], can also be determined by way of finite element calculation. In order to do this, a total number of n calculations are necessary, wherein for each calculation a geometrical imperfection with a size of “1” is assumed for each of the considered cross-sections alternately. This theoretical imperfection decreases linearly between the neighboring cross-sections. By once again subtracting the normally occurring stresses from the stress field and by calculating the difference between mean stresses in both flanks, all values of the matrix [H] can be calculated. The element, $h_{i,j}$, of the matrix is then, based on a calculation with only imperfections in cross-section j, related to the stresses in cross-section i:

$$h_{i,j} = \left(\sigma_{i,j} - \sigma_{i,perfect,j}\right)_{left} - \left(\sigma_{i,j} - \sigma_{i,perfect,j}\right)_{right} \tag{2}$$

The problem of determining the geometrical imperfections is thus reduced to solving a system of n equations in n unknowns which can be done quite easily.

4 PRACTICAL APPLICATION ON THE ALBERT CANAL BRIDGE

The mean stress difference between both flanks of the arch cross-section of the Albert Canal Bridge, based on strain gauge measurements is:

$$(\sigma) = \begin{pmatrix} -0.28 \\ 0.45 \\ -1.01 \\ -0.64 \\ -0.85 \\ -0.33 \end{pmatrix} \tag{3}$$

Based on the calculated stress field in a perfect arch (Figure 6, left) and six calculations with an out-of-plane imperfection of "1" in each cross-section alternatively (Figure 6, right), matrix [H] can be determined:

$$(\sigma) = \begin{pmatrix} -6.99 & 3.13 & 0.73 & -0.22 & -0.32 & -0.41 \\ 3.37 & -6.62 & 2.99 & 0.00 & 0.16 & -0.11 \\ 0.71 & 2.94 & -5.68 & 3.21 & 0.18 & 0.15 \\ -0.15 & 0.18 & 3.21 & -5.67 & 2.92 & 0.71 \\ -0.11 & 0.16 & 0.00 & 2.99 & -6.62 & 3.35 \\ -0.42 & -0.33 & -0.23 & 0.76 & 3.23 & -7.27 \end{pmatrix} \tag{4}$$

The unknown out-of-plane imperfection will then be (cm):

$$(\delta) = (H)^{-1}(\sigma) = \begin{pmatrix} 1.08 \\ 2.15 \\ 3.62 \\ 3.69 \\ 2.47 \\ 1.25 \end{pmatrix} \tag{5}$$

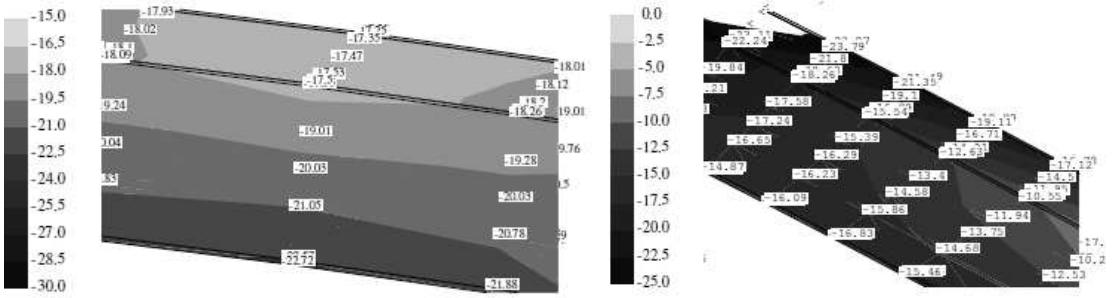

Figure 6. Stresses in a perfect arch bridge (left) and in a bridge with an imperfection of "1" in the first cross-section [MPa].

These values are also shown in Figure 7 (left), as well as an extrapolated overall imperfection shape. In this and all following graphs, the horizontal axis represents the span length (m) and the vertical axis the geometrical out-of-plane imperfections (mm). An upper and lower margin is derived based on the measurement precision of the strain gauge data acquisition system. The shape is more or less sinusoidal and the maximal amplitude stays well below 45mm, while the to be expected value, according to ECCS would be about 117mm (or one 1000th of the span length).

5 GEOMETRICAL IMPERFECTIONS OF OTHER BRIDGES

As shown in Figure 7 (right), the shape of the imperfections of the IJzerlaan Bridge is also more or less sinusoidal. The imperfection is directed towards the deck and the other

arch of the bridge. The maximal value is furthermore considerably smaller as was to be expected based on design codes.

The imperfections of the Kapelse Steenweg Bridge are shown in Figure 8. The size of the imperfections is quite small, less than 20mm, while the shape is quite symmetrical. In addition, the shape seems quite logical when looking at the construction method. The arch was assembled in three separate parts. Both arch springs were erected first, while the entire middle portion of the arch was introduced afterwards. This results in maximal imperfection in the middle region and discontinuities in the zones where the three parts are connected. The out-of-plane imperfection of the Bredabaan Bridge, which is identical to the one crossing the Kapelse Steenweg, is shown in Figure 8. Nevertheless, all values much lower and the overall shape is less sinusoidal. This bridge was assembled differently: the left part was the last one to be assembled, resulting in the imperfection being more pronounced there.

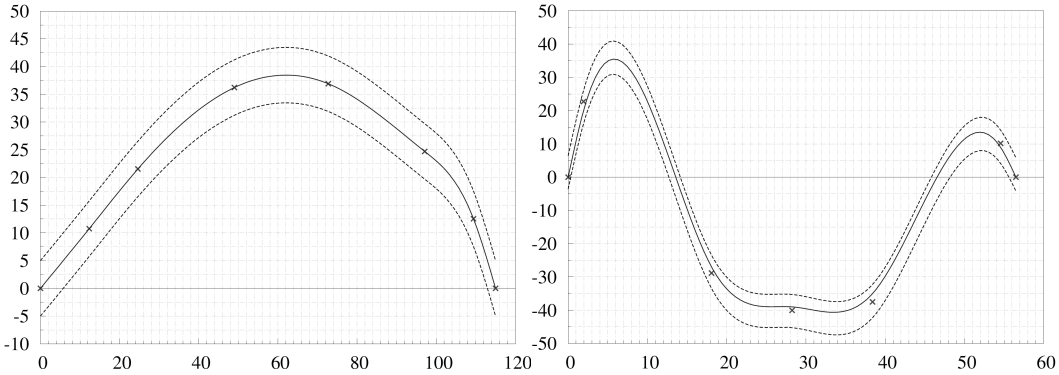

Figure 7. Geometrical out-of-plane imperfections of the Albert Canal bridge (left) and IJzerlaan bridge (right) [mm].

Figures 9 and 10 display the geometrical imperfections of the much larger bridges in Schaarbeek and Prester. Both imperfection shapes are sinusoidal along the entire length of the span. The only deviation is close to the arch springs where the stress field is more complex. Although both bridges are identical, the size of the imperfections of the Prester Bridge is about 20 mm higher than the Schaarbeek Bridge. The difference is once more caused by the construction technique. While all connections of the Schaarbeek Bridge are welded, the Prester Bridge is bolted, resulting in drastically higher imperfections. The Prester Bridge was also topographically measured. Surveyors could set up in the valley under the bridge, perpendicular to the bridge at a distance of about 150m. The resulting out-of-plane deformations of the arch are the additional lines in figure 10. The shape and size of the imperfections are almost perfectly identical.

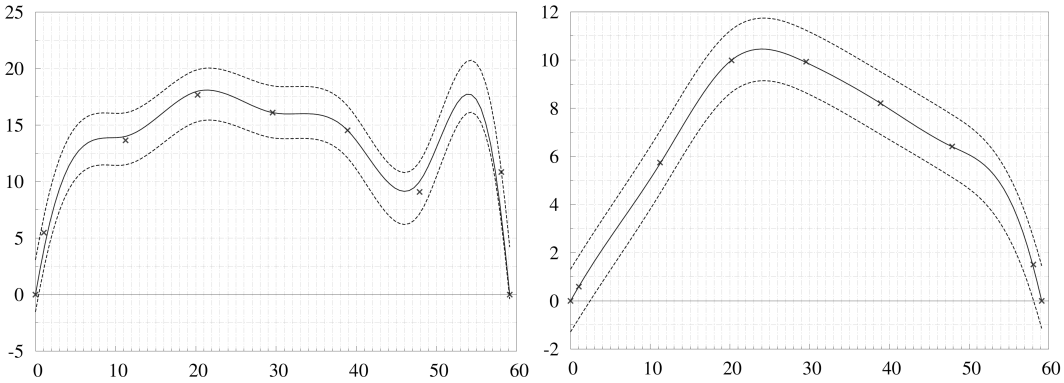

Figure 8. Geometrical out-of-plane imperfections of the Kapelse Steenweg(left) and Bredabaan (right) bridge [mm].

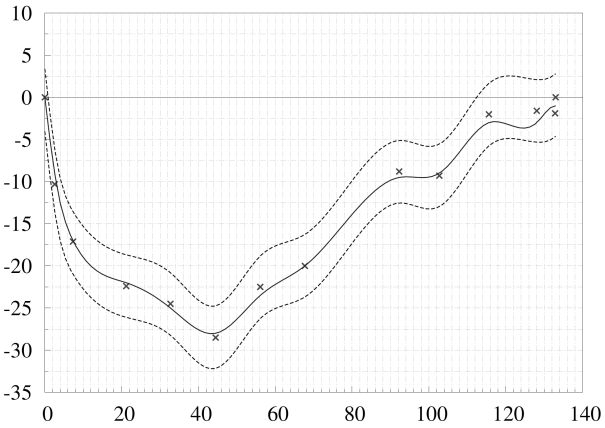

Figure 9. Geometrical out-of-plane imperfections of the Schaarbeek bridge [mm].

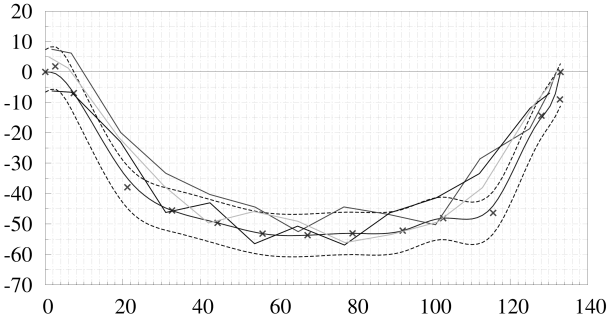

Figure 10. Geometrical out-of-plane imperfections of the Prester bridge [mm].

6 CONCLUSIONS

Six bridges in total have been equipped with strain gauges along their entire length. For the actual determination of the imperfection, a detailed finite element model has been developed, describing all internal forces in an arch bridge, such as normal force, in-plane and out-of-plane bending and torsion, separately. In addition, the detailed model takes the influence of deformations on the internal forces into account. This method is verified using the results of topographical measurements of some of the studied bridges. Both sets of results are in agreement when it comes to size and shape of the imperfections. The shape of the resulting geometrical imperfection is for most of these bridges a half sine wave. The most important result is however that for all bridges the

size of the imperfections is substantially smaller than the one predicted by the Eurocodes.

7 REFERENCES

O'Connor, C., "Design of bridge superstructures". New York: John Wiley & Sons, Inc., 1971

Xanthakos, P.P.," Theory and design of bridges". New York: John Wiley & Sons, Inc. , 1994

Van Bogaert, Ph., Outtier A., "Experimental verification of lateral buckling of steel tied arch bridge", 6th International symposium on steel bridges, Prague, 2006